Influence of self-healing property of Ultra-High Performance Concrete under aggressive environment

Bin Xi*, *Liberato* Ferrara
Department of Civil and Environmental Engineering
Politecnico di Milano
Piazza Leonardo da Vinci 32, 20133 Milano, Italy

Abstract. This paper investigates the evolution of self-healing properties of ultra-high performance concrete exposed to aggressive environments. Double edge wedge splitting UHPC specimens with 0.8% crystalline admixture and 1.5% steel fibre by volume have been first pre-cracked up to a average 0.30 mm crack opening displacement (COD) obtained by two linear variable differential transformers attached to both sides of the sample surface. Then, the pre-cracked samples have been exposed to three different environments: tap water, salt water (a NaCl aqueous solution at 3.3% concentration) and geothermal water obtained from a geothermal power plant. After one month exposure, samples were carried out re-crack to know the self-healing properties. The results from ultrasonic pulse velocity tests (UPV) reveal that the samples exposed to tap water exhibit the highest rate of recovery along the exposure time, while those exposed to geothermal water show the lowest. The calculated indexes of cracking self-healing (ICS) show a 73.8% closure in tap water, 58.4% in salt water 43.9% in geothermal water. Additionally, the index of damage recovery, evaluated from UPV frequencies as well as from the stress vs. COD curves of pre-cracking and post-healing re-cracking tests on specimens, and the equivalent tensile stress also indicate a higher level of healing capable of inducing a significant recovery of mechanical properties.

1 Introduction

In recent years, Ultra-High Performance Concrete (UHPC) has gained significant attention as an advanced concrete material [1]. According to the ACI Committee 239 report [2], UHPC boasts a compressive strength of over 150 MPa after 28 days. Additionally, due to steel fibres, it has enhanced tensile properties and exceptional crack control which can result into tensile strain hardening response. The tensile ultimate strain can approach the yield strain of steel reinforcement (0.2%) and the material is distributing an otherwise localized damage into stably growing multiple narrow cracks, with widths of 0.02 to 0.03 mm [3]. To achieve the aforesaid outstanding mechanical property, UHPC features a low water-cement ratio, a high amount of fine aggregate and fine reactive powder, resulting in a dense internal structure, making it more resistant to cracking and durable than conventional concrete [1]. However, the majority of the studies that have been published to date have focused exclusively on the properties of intact and non-cracked UHPC [4]. In fact, UHPC is also subject to a significant risk of cracking. This is due, on the one hand, to cracking caused by changes in load, temperature and humidity during the service life of UHPC structures, and, on the other hand, to the high autogenous shrinkage of UHPC from the use of high doses of cement, which can induce, if restrained, microcracking at very early ages [5]. Cracked UHPC structures often work in aggressive environments, exactly due to the potential high durability of the material, where large amounts of aggressive ions can enter the interior of the UHPC structure through the cracks and attack the cement matrix and both the fibers and the ordinary reinforcement, if any [6]. This can jeopardize the long-term performance of the structure and the characteristics of UHPC are not fully exploited. Therefore, improving the performance of cracked UHPC has started becoming a challenging research topic in recent years. Self-healing techniques are considered to be one of the most promising solutions to this issue. UHPC has a natural ability to close cracks due to the continuous hydration reaction of cement particles and the carbonation of hydration products. Additionally, researchers have also been able to enhance UHPC's self-healing ability by adjusting the type and amount of supplementary cementitious materials (SCMs), adding crystalline admixtures (CA) [7], or using various autonomous self-healing technologies including encapsulated polymeric healing agents [8], expansive agents [9], and macro-capsules with bacteria [10].

In this study, the self-healing performance of UHPC containing a commercial CA (Penetron Admix ®)in three different healing exposures was examined. Pre-cracked UHPC samples were exposed to three types of water: tap water, salt water, and geothermal water.

* Corresponding author: bin.xi@polimi.it

Optical microscopy was utilized to record the crack closure after different curing periods and ultrasonic pulse velocity (UPV) and splitting tensile tests, tailored to the Double Edge Wedge Splitting geometry of the specimens, have been conducted to determine the recovery of mechanical properties.

2 Materials and test methods

2.1 Materials

Table 1 shows the mixture proportion of UHPC. The specific procedure for preparing the UHPC can be found in the authors' previous publications [11].

2.2 Preparation of the pre-cracked samples

UHPC was cast into large slabs and cut into 500×100×50 mm beams and stored at a temperature of 20°C and 90% humidity for up to one year to minimize the effect of delayed hydration on self-healing properties. These beam samples were then precisely cut into double edge wedge splitting (DEWS) samples as shown in Fig. 1. It has been previously demonstrated that this test methodology, especially for UHPC, provides a good understanding of the relationship between tensile stress and crack opening displacement (COD) [12]. The DEWS samples were first subjected to pre-cracking, in displacement-controlled mode at a rate of 0.005 mm/s. Fig. 2 shows the linear variable differential transformers (LVDTs) attached to both sides of the sample surface recorded the crack opening displacement at the middle sides during loading. When the average COD obtained by LVDTs is up to a 0.30 mm, the unloading test could be carried out with same loading speed, thus obtaining the full loading and unloading curve of the sample. The average crack width of the final samples was found to be between 30-150 µm due to removal of the loading. After pre-cracking tests, the cracked samples were immersed in three different water environments: tap water, salt water and geothermal water. The tap water was taken from the water supply network of the city of Milan; the prepared salt water had a concentration of 3.3%; the geothermal water was taken from a geothermal power plant in Chiudino, Tuscany. Table 2 shows the chemical composition of the geothermal water, with a high content of sulfates and chlorides.

Table 1. Mixture proportions of UHPC

Constituents (kg/m^3)						
CEMI 52.5 R	Slag	Water	Steel fibers	Sand 0-2mm	SP	CA
600	500	200	120	982	33	4.8

Table 2. Composition of the geothermal water (in ppm)

Al	Ca	Fe	K	Mg
0.2	4	0.13	19.8	0.3
Na	S	Si	SO_4^{2-}	Cl
1243	1523	0.3	2678	441

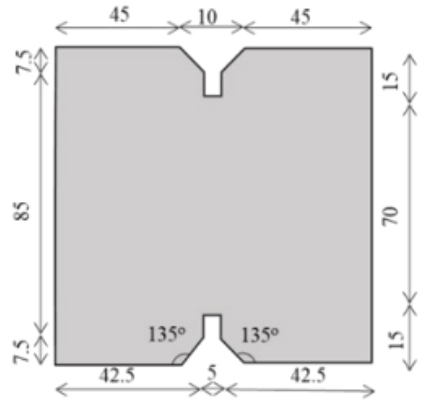

Fig.1. Dimensions of the DEWS specimens

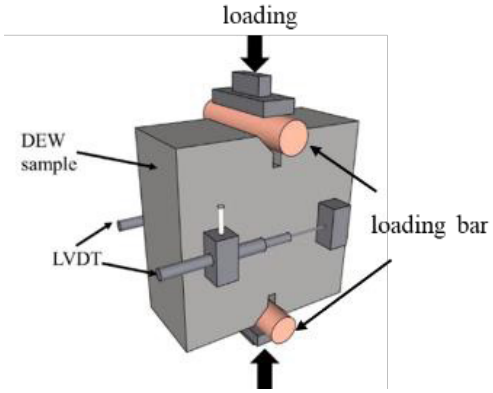

Fig.2. Scheme of pre-crack test

2.3 Microscopic Techniques for the evaluation of Crack Closure

The cracks of sample were captured at different curing times using a digital optical microscope and the software DinoLite Capture . The acquired photos were transferred into Phothoshop® to reconstruct the whole crack, as shown in Fig. 3. The area A_{area} and crack length l_{length} were computed using the mathematical and statistical tool of Phothoshop®. A_{area} divided by l_{length} has been assumed equal to the average crack width. The index of crack self sealing (ICS) was computed as per Eq.1 to evaluate the crack self-sealing capacity.

$$Index\ of\ crack\ self\ sealing = \frac{w_{initial} - w_{after\ sealing}}{w_{initial}} \quad (1)$$

Where $w_{initial}$ is the initial crack width; $w_{after\ sealing}$ is the crack width after the specimen remained immersed for the scheduled time in the different water environments.

2.4 Ultrasonic pulse velocity test

The UPV test is commonly used to evaluate concrete damage and self-healing capabilities [13]. The speed of acoustic waves between the emitter and the receiver is affected as the crack's depth and width vary. For the test, the transmission distance between the transmitter and receiver was 100 mm; the diameter of the transducer was 50 mm; the signal frequency was 50 kHz. The wave velocity has been calculated by the distance between the emitter and the receiver divided by the time of wave transmission from the sample. The tests were conducted

on samples that were undamaged (UPV_0), pre-cracked and healed (UPV).

2.5 Re-cracking test

UHPC DEWS samples were be subjected to cracking-healing cycles test. The test followed the procedure: after 1 month of sample exposure (for each of the three exposure conditions), re-cracking up to 0.3 mm. **Fig. 4** shows this healing-cracking cycle scheme. The current study implemented a re-cracking test after one month of exposure.

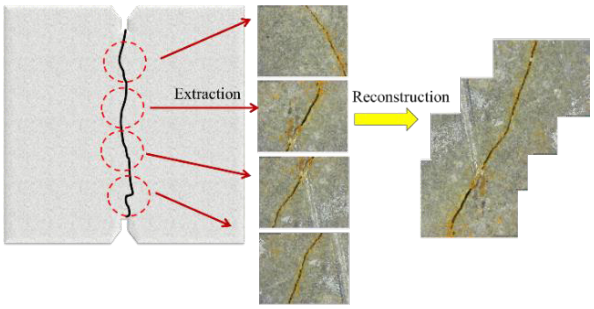

Fig. 3. Schematics of the procedure for crack imaging and crack width calculation

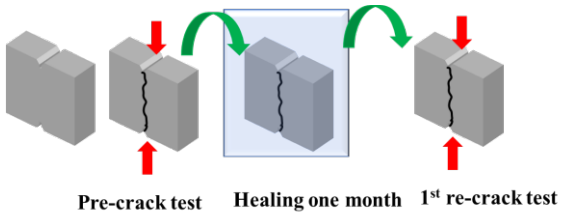

Fig. 4. Scheme of cracking-healing cycles

3 Results and Discussions

3.1 Index of Crack Sealing

According to **Eq. 1**, the ICS of pre-cracked samples in different water environments for 7, 14, 21 and 28 days was calculated. **Fig. 6** shows the ICS results and **Fig.7** provides images of cracks closure. At seven days, the ICS for samples exposed to tap water, salt water, and geothermal water were 47.8%, 30.9%, and 27.2%, respectively. As the healing period increased to 1 month, their ICS significantly increased, with tap water at 73.8%, salt water at 58.4%, and geothermal water at 43.9%. Exposure to tap water resulted into better sealing than exposure to saltwater and geothermal water. In fact, the closure of cracks mainly comes from the continued hydration of cement and the action of CA [14]. CA can combine with hydration products to form healing products that can deposit and repair cracks. Previous studies have also shown that the healing products are mainly $CaCO_3$ [15]. The presence of chloride ions in saltwater and sulfate and chloride ions in geothermal water may not be conducive to the generation of self-healing products $CaCO_3$, resulting in lower crack sealing levels [16].

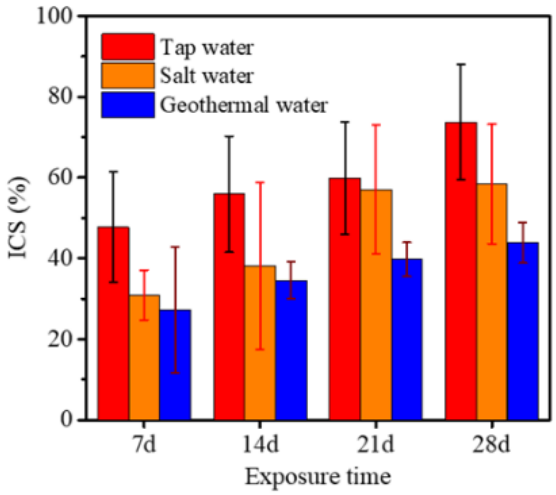

Fig. 6. Comparison of ICS in difference water environments and healing time

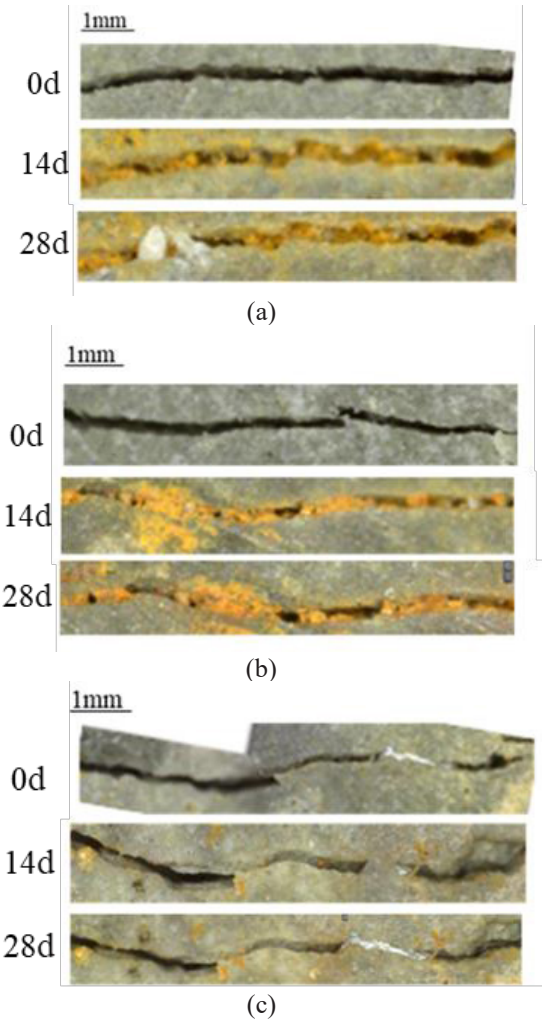

Fig. 7. Images of cracks closure in different environments (a)tap water; (b)salt water;(c) geothermal water

3.2 UPV tests

Fig. 8 presents the temporal evolution of the UPV/UPV_0 ratio, which represents the ultrasonic pulse velocity at different times after pre-cracking and healing as referred to its value on undamaged samples. This ratio serves as

an indicator of the healing extent of the sample under varying exposure times and water environments.

As the duration of exposure time increases, a gradual increase in the UPV/UPV$_0$ ratio is observed, which subsequently stabilizes. It is noteworthy that samples exposed to tap water display the highest level of recovery, while those exposed to geothermal water exhibit the lowest. This trend is in line with the findings of the ICS analysis.

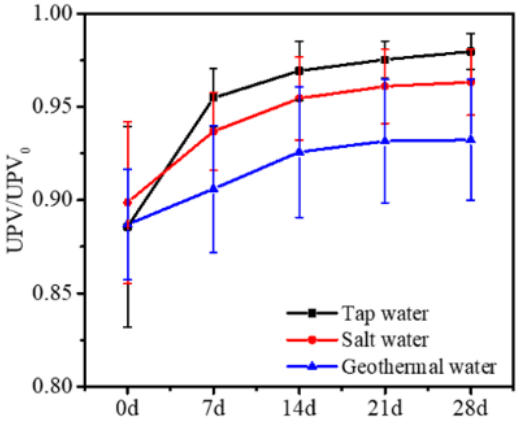

Fig. 8. The UPV/UPV$_0$ ratio with different days

3.3 Mechanical properties recovery

From the stress vs. Crack Opening Displacement (COD) curves, obtained from pre-cracking and post- healing re-cracking tests on DEWS samples, the recovery of mechanical properties was studied by calculating the Index of Damage Recovery (IDR) and equivalent post-healing re-cracking tensile stress σ_{eq}. The procedure is outlined in Fig. 9 and Eq. 2 and Eq. 3 respectively. Equivalent post-healing re-cracking tensile stress is calculated as the work of fracture divided by the change in crack width [17].

$$\text{IDR} = \frac{K_{loading,\ recracking} - K_{unloading,precracking}}{K_{loading,\ precracking} - K_{unloading,precracking}} \quad (2)$$

Where $K_{unloading,precracking}$ is initial unloading stiffness; $K_{loading,\ precracking}$ is initial loading stiffness; $K_{loading,\ recracking}$ is re-cracking stiffness.

$$\sigma_{eq}[MPa] = {W_F[MPa.mm]}\Big/{(w_{max} - w_{min})[mm]} \quad (3)$$

Where W_F is the absorbed energy per unit cracking, as also highlighted in Fig. 9.

As illustrated in Fig. 10, the samples exposed to tap water exhibit the highest IDR of 21.4% and equivalent tensile stress of 12 MPa, while those exposed to geothermal water have the lowest IDR of 9.6% and equivalent tensile stress of 9.1 MPa. The samples exposed to tap water display the highest level of self-healing, resulting in a superior level of mechanical property recovery.

The recovery of mechanical properties has a strong correlation with the level of self-healing. As shown in Fig.11, the relationship between ICS and UPV/UPV$_0$, as well as the equivalent tensile stress σ_{eq} and IDR at 28 d, are depicted. A higher ICS results in an improvement of all three indicators. However, the effect on UPV/UPV0 is not very pronounced. The effect of ICS on the recovery of mechanical properties is significant. Specifically, an ICS of 73.8% in tap water results in σ_{eq} and IDR that are 31.5% and 123.4% higher than an ICS of 43.9% in geothermal water. Both values are also 22.7% and 76.9% higher than an ICS of 58.4% in salt water.

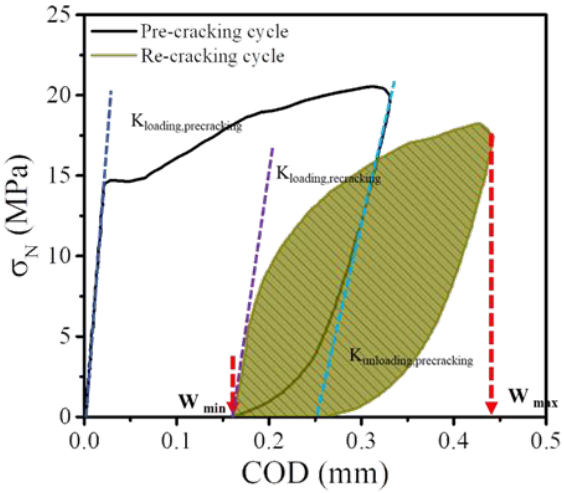

Fig.9. Example of tensile stress (σ_N) versus COD curves. Methodology definition to obtain the absorbed energy per unit fracture surface (WF), and $K_{unloading,precracking}$, $K_{loading,\ precracking}$ and $K_{loading,\ recracking}$.

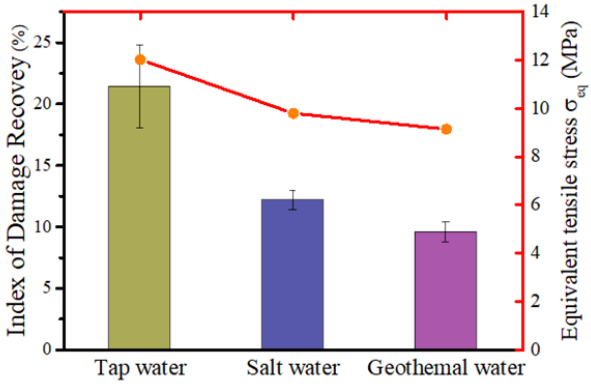

Fig.10. The results of IDR and equivalent tensile stress

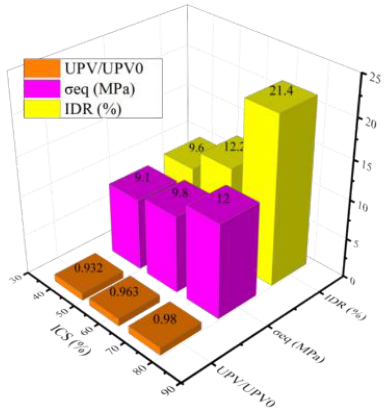

Fig.11.The relationship between ICS and UPV/UPV$_0$, σ_{eq} and IDR

4 Conclusion

This study presents a preliminary examination in which cracked UHPC samples were exposed to various environments, including tap water, salt water, and geothermal water, in order to assess the healing capabilities in these scenarios and upon successive cycles of healing and (re-)cracking after one month exposure. The key results of this study can be outlined as follows:

1. The results of ICS reveal that the cracks in the samples healed continuously with increasing exposure time. Specifically, when immersed in tap water, the healing level is the highest at 47.8% after 7 days, and 73.8% after 1 month. However, when exposed to geothermal water, the self-healing level is the lowest, with the ICS barely reaching 50% even in one month.

2. The UPV results show that samples exposed to salt water and geothermal water recovered at lower average velocities than samples exposed to tap water. Moreover, samples exposed to geothermal water have the lowest velocity recovery.

3, The results of the recovery of mechanical properties revealed that the samples exposed to tap water had the highest IDR (21.4%) and equivalent tensile stress (12 MPa). Conversely, the samples exposed to geothermal water had the lowest IDR of 9.6% and equivalent tensile stress of 9.1 MPa. This is because samples exposed to tap water have higher ICS than other exposure conditions. The result presents a strong correlation between the recovery of mechanical properties and the self-healing level.

The research activity reported in this paper has been performed in the framework of the ReSHEALience project (Rethinking coastal defense and Green-energy Service infrastructures through enHancEd-durAbiLity high-performance cement-based materials) which has received funding from the European Union's Horizon 2020 research and innovation program under grant agreement No 760824. Bin Xi also acknowledges the financial support of the China Scholarship Council (CSC) under the grant agreement No.202008440524 for PhD study in Structural Geotechnical and Earthquake Engineering at Politecnico di Milano.

References

[1] C. Shi, Z. Wu, J. Xiao, D. Wang, Z. Huang, Z. Fang, Constr. Build. Mater. **101** (2015) 741.
[2] ACI Committee 239, Am. Concr. Inst. (2018).
[3] Z. Zhou, P. Qiao, J. Test. Eval. **48** 4 (2020) 20170644.
[4] M.A. Bajaber, I.Y. Hakeem, J. Mater. Res. Technol. **10** (2021) 1058.
[5] S. Park, S. Wu, Z. Liu, S. Pyo, Materials (Basel). **14** 6 (2021) 1472.
[6] S. Al-Obaidi, M. Davolio, F. LO Monte, F. Costanzi, M. Luchini, P. Bamonte, L. Ferrara, Case Stud. Constr. Mater. **17** May (2022) e01202.
[7] F. Lo Monte, L. Ferrara, Constr. Build. Mater. **283** (2021) 122579.
[8] B. Hilloulin, K. Van Tittelboom, E. Gruyaert, N. De Belie, A. Loukili, Cem. Concr. Compos. **55** (2015) 298.
[9] Y.-S. Wang, H.-S. Lee, R.-S. Lin, X.-Y. Wang, J. Build. Eng. **50** (2022) 104230.
[10] D. Zhang, M.A. Shahin, Y. Yang, H. Liu, L. Cheng, J. Build. Eng. **50** (2022) 104132.
[11] S. Al-Obaidi, P. Bamonte, F. Animato, F. Lo Monte, I. Mazzantini, M. Luchini, S. Scalari, L. Ferrara, Sustainability **13** 17 (2021) 9826.
[12] M. di Prisco, L. Ferrara, M.G.L. Lamperti, Mater. Struct. **46** 11 (2013) 1893.
[13] Y. Zhang, R. Wang, Z. Ding, Materials (Basel). **15** 2 (2022) 440.
[14] M. Nasim, U.K. Dewangan, S. V. Deo, Mater. Today Proc. **32** (2020) 638.
[15] N. De Belie et al., Adv. Mater. Interfaces **5** 17 (2018) 1800074.
[16] B. Xi, Z. Huang, S. Al-Obaidi, F. LO Monte, L. Ferrara, fib Symp. September (2022) 329.
[17] E. Cuenca, L. Ferrara, Theor. Appl. Fract. Mech. **106** (2020) 102468.